Virtual MG meeting 2021

Mirror Dark Matter searches in laboratory and in sky

… and sorry for a different title …

Andrea Addazi, Sichuan University,
INFN LNF Frascati

Mirror Dark Matter is the most elegant candidate.

It is a natural prediction of restauration of parity symmetry in the standard model.
We do not introduce any new free parameters.

Logically simple,
Occam's razor on the lagrangian
rather than number of particles.

Doubling of degrees of freedom,
High dark astrophysical complexity…
Dark Matter and lensing?
Subtle but not malicious…

Mirror Parity

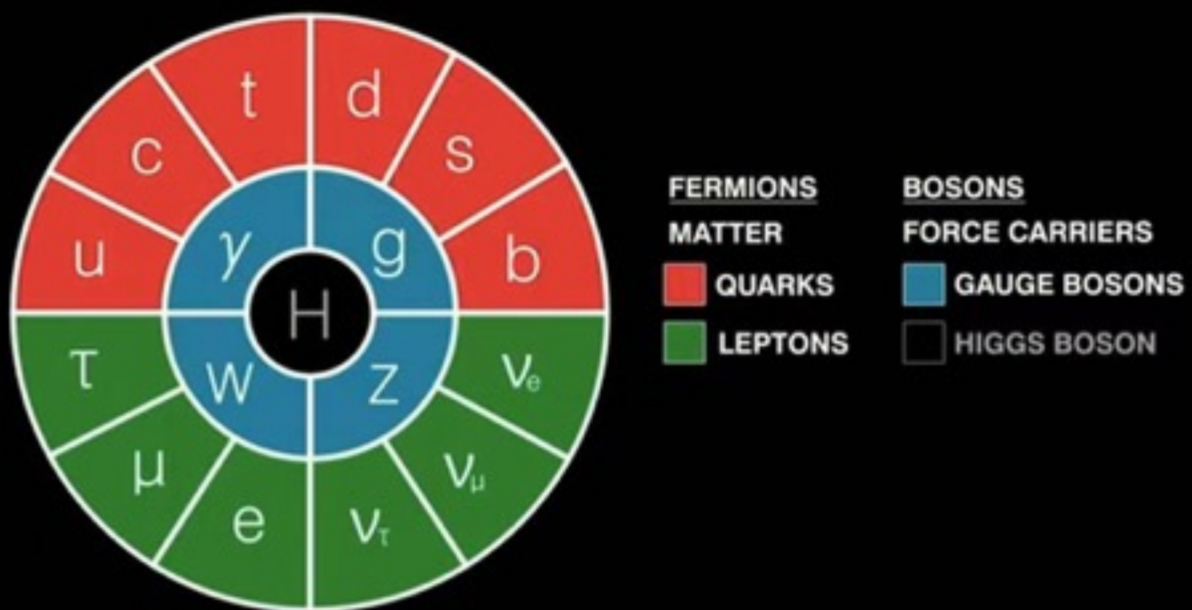

V-L Ordinary weak interactions

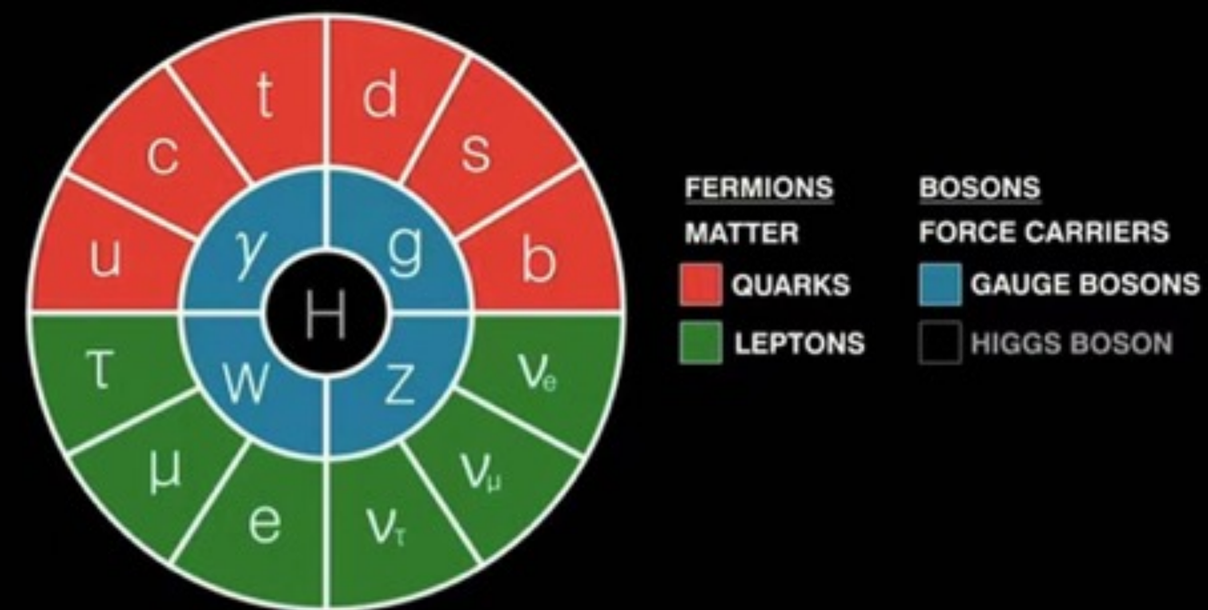

V+L Mirror weak interactions

a brief history of Mirror Matter

T.D. Lee and C.N. Yang 1956, Nobel prize paper

Kobzarev, Okun and Pomeranchuk 1966

S. Blinnikov and M. Khlopov 1983

Z. Berezhiani et al, R. Foot et al, for a massive investigation of cosmological implications

Mirror Parity can be preserved or spontaneously broken. Phenomenology is different

see Z. Berezhiani (2005) “Through the looking-glass: Alice’s adventures in mirror world,” In From Fields to Strings, Circumnavigating Theoretical Physics, Eds. M. Shifman et al., vol. 3, pp. 2147-2195 [arXiv:hep-ph/

Relevant Renormalizable portals

O- M- Higgs mixing $$\mathcal{V}_{\rm mix} = \kappa(\phi^\dagger\phi)(\phi'^\dagger\phi')$$

Cosmological limits $$\bar\phi\phi \to \bar\phi'\phi'$$ $$\kappa < 10^{-8}$$

O-M-photon kinetic mixing $$\mathcal{L} = -\varepsilon F^{\mu\nu}F'_{\mu\nu}$$

orthopositronium limits $$e^+e^- \to e'^+e'^-$$ $$\varepsilon < 3\times10^{-7}$$

CMB distortion: 2 orders below

…And of course they are directly interacting through gravity

Effective higher order operators

D=9 O-M-quark mixings

$$\frac{1}{\mathcal{M}^5}\overline{(u'd'd')}_L(udd)_R \;+\; \text{h.c.}$$

Inducing O-M neutron mixings, compatible with Cosmological limits if M=10 TeV

$$\varepsilon\, \overline{n'}n + \text{h.c.}$$

$$\varepsilon \simeq \frac{\Lambda^6_{\text{QCD}}}{\mathcal{M}^5} \simeq \left(\frac{10\ \text{TeV}}{\mathcal{M}}\right)^5 \times 10^{-15}\ \text{eV}$$

$$\varepsilon \sim 10^{-15}\ \text{eV}$$

Weinberg's ode and O-M-neutrino mixings

$$\frac{1}{M}\phi l D l' \phi' + \text{h.c.}$$

$$(n \to n')$$

Cosmology of the Mirror sector

Ordinary and Dark Matter coincidence problem: 1:5.
Dark particles not so different than Baryons

O- and M- worlds must have the same microphysics but different cosmological histories. Different temperatures after inflation reheating. How?
Berezhiani's mechanism:
Higgs-Leptons collisions through RH-neutrinos.
O- and M- can only have non-gravitational very weak couplings.
Thus, Mirror BBN is different and we expect more He'-4…
Structure and stars formations drastically different!

Mirror neutrinos as sterile? Their counting is suppressed by the hierarchy of the O- M- temperatures

see Z. Berezhiani (2005) "Through the looking-glass: Alice's adventures in mirror world," In From Fields to Strings, Circumnavigating Theoretical Physics, Eds. M. Shifman et al., vol. 3, pp. 2147-2195 [arXiv:hep-ph/0508233]

Symmetric Mirror Dark Matter

No in colliders. Attempts by Foot et al incompatible with Cosmological limits from re-thermalization

Direct Detection. Possible from photon mirror photon kinetic mixing. Different interactions and signals than WIMPS or other chimeras (for example leptophilic DM)

Ultra Cold Neutron Physics or Neutron baselines

Neutrino oscillations, unitarity and short baselines

However, it is also possible that Mirror and Ordinary worlds do not have any non-gravitational interactions. In this case, the only way to search Mirror matter is through gravitational lensing or gravitational waves!

New Possibilities from Gravitational waves. Dark Neutron stars mergings

Mirror Matter and Baryon violations

Neutron-antineutron physics

D=9 6 quark ope,
3 years in vacuum
limit ’97
Baldo-Coelin

Neutron-Antineutron: Mirror short-cut

$$n \to n'/\overline{n}' \to \overline{n}$$

Berezhiani's model *(see for example last 2021 paper)*

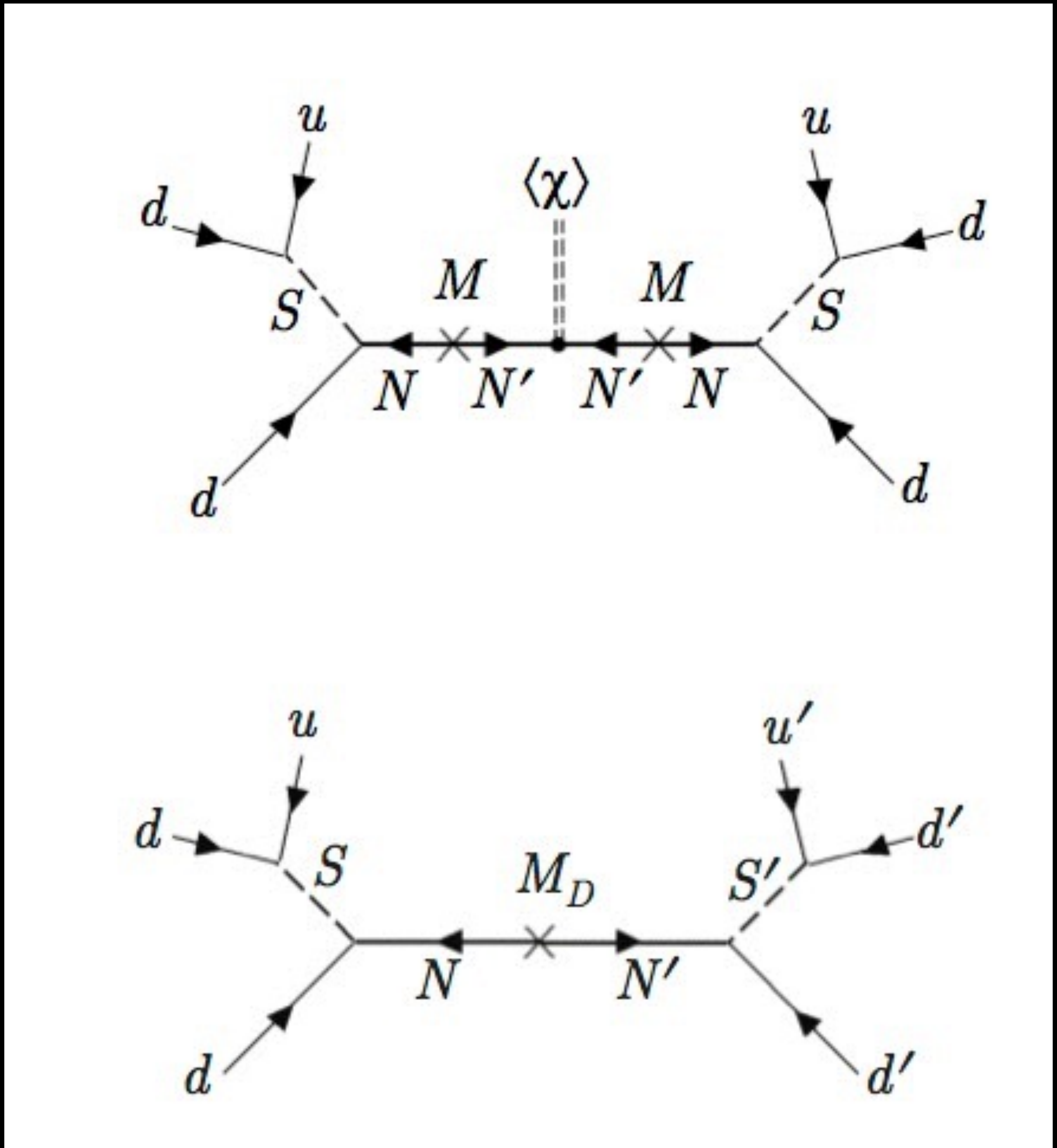

Complementary searches in UCN

…

Possible anomaly, Serembrov’s group (see *Berezhiani&Nesti)*

New high-sensitivity searches for neutrons converting into antineutrons and/or sterile neutrons at the European Spallation Source

A. Addazi[h,at], K. Anderson[aq], S. Ansell[bm], K. S. Babu[az], J. Barrow[w], D. V. Baxter[d,e,f], P. M. Bentley[ac], Z. Berezhiani[b,l], R. Bevilacqua[ac], R. Biondi[b], C. Bohm[ba], G. Brooijmans[an], L. J. Broussard[aq], B. Dev[ay], C. Crawford[z], A. D. Dolgov[ai,ao], K. Dunne[ba], P Fierlinger[o], M. R. Fitzsimmons[w], A. Fomin[n], M. Frost[aq], S. Gardiner[c], S. Gardner[z], A. Galindo-Uribarri[aq], P. Geltenbort[p], S. Girmohanta[bb], E. Golubeva[ah], G. L. Greene[w], T. Greenshaw[aa], V. Gudkov[k], R. Hall-Wilton[ac], L. Heilbronn[x], J. Herrero-Garcia[be], G. Ichikawa[bf], T. M. Ito[ab], E. Iverson[aq], T. Johansson[bg], L. Jönsson[ad], Y-J. Jwa[an], Y. Kamyshkov[w], K. Kanaki[ac], E. Kearns[g], B. Kerbikov[al,aj,ak], M. Kitaguchi[ap], T. Kittelmann[ac], E. Klinkby[ae], A. Kobakhidze[bl], L. W. Koerner[s], B. Kopeliovich[bi], A. Kozela[y], V. Kudryavtsev[ax], A. Kupsc[bg], Y. Lee[ac], M. Lindroos[ac], J. Makkinje[an], J. I. Marquez[ac], B. Meirose[ba,ad], T. M. Miller[ac], D. Milstead[ba,*], R. N. Mohapatra[j], T. Morishima[ap], G. Muhrer[ac], H. P. Mumm[m], K. Nagamoto[ap], F. Nesti[l], V. V. Nesvizhevsky[p], T. Nilsson[r], A. Oskarsson[ad], E. Paryev[ah], R. W. Pattie, Jr.[t], S. Penttilä[aq], Y. N. Pokotilovski[am], I. Potashnikova[bi], C. Redding[x], J-M. Richard[bj], D. Ries[af], E. Rinaldi[au,bc], N. Rossi[b], A. Ruggles[x], B. Rybolt[u], V. Santoro[ac], U. Sarkar[v], A. Saunders[ab], G. Senjanovic[bd,bn], A. P. Serebrov[n], H. M. Shimizu[ap], R. Shrock[bb], S. Silverstein[ba], D. Silvermyr[ad], W. M. Snow[d,e,f], A. Takibayev[ac], I. Tkachev[ah], L. Townsend[x], A. Tureanu[q], L. Varriano[i], A. Vainshtein[ag,av], J. de Vries[a,bh], R. Woracek[ac], Y. Yamagata[bk], A. R. Young[as], L. Zanini[ac], Z. Zhang[ar], O. Zimmer[p]

[a]*Amherst Center for Fundamental Interactions, Department of Physics, University of Massachusetts, Amherst, MA, USA*
[b]*INFN, Laboratori Nazionali del Gran Sasso, 67010 Assergi AQ, Italy*
[c]*Fermi National Accelerator Laboratory, Batavia, IL 60510-5011, USA*
[d]*Department of Physics, Indiana University, 727 E. Third St., Bloomington, IN, USA, 47405*
[e]*Indiana University Center for Exploration of Energy & Matter, Bloomington, IN 47408, USA*
[f]*Indiana University Quantum Science and Engineering Center, Bloomington, IN 47408, USA*
[g]*Department of Physics, Boston University, Boston, MA 02215, USA*
[h]*Center for Theoretical Physics, College of Physics Science and Technology, Sichuan University, 610065 Chengdu, China*

Tests of new interactions and weak gravity conjecture

$$V_i = \alpha_{B-L}\frac{Q_i Q_A}{r}e^{-r/\lambda}, \qquad \lambda = \frac{1}{M_b} \simeq \left(\frac{10^{-49}}{\alpha_{B-L}}\right)^{1/2}\left(\frac{1\ \mathrm{keV}}{v}\right) \times 0.6\cdot 10^{16}\ \mathrm{cm}$$

$$M_b = 2\sqrt{2}gv, \qquad v = \left[v_\chi^2 + (Q_i/Q_\chi)^2 v_i^2\right]^{1/2} \geq v_\chi$$

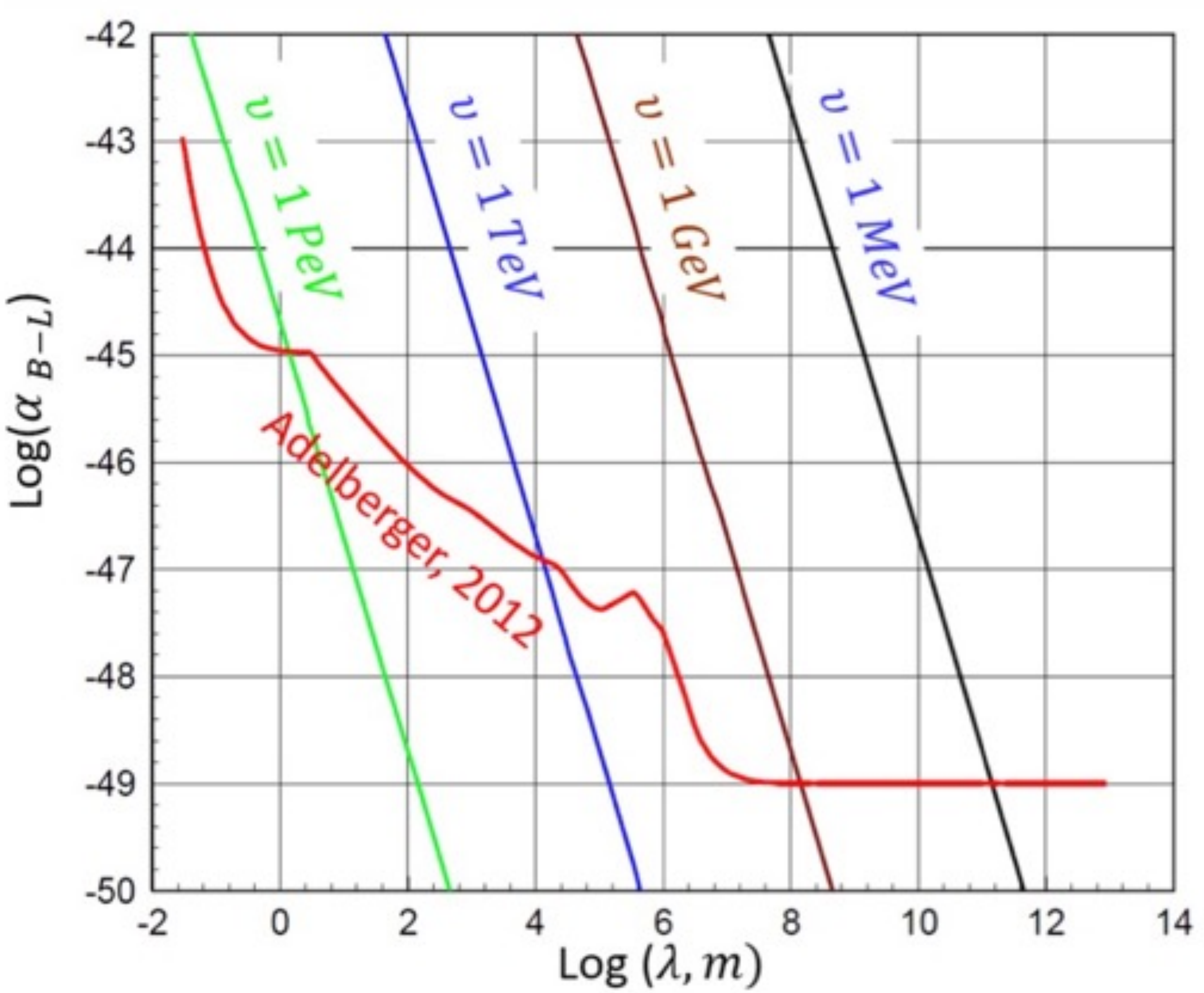

Addazi, Berezhiani, Kamhyskov (2015), Addazi (2017)

Gravitational waves

Mirror matter trapped in Ordinary Neutron stars and Equation of state modified
recently Berezhiani et al, Ciancarella, Pannarale, Addazi, Marciano).
n-n' oscillations

We inspect the possibility that neutron star interiors are a mixture of ordinary matter and mirror dark matter. This is a scenario that can be naturally envis- aged according to well studied accretion mechanisms, including the Bondi-Hoyle one. We show that the inclusion of mirror dark matter in neutron star models lowers the maximum neutron star mass for a given equation of state, and that it decreases the tidal deformability of a given neutron star. These general fea- tures imply that, given an equation of state, one can constrain the maximum viable amount of mirror dark matter in neutron stars in order to consistently fulfill existing maximum mass and tidal deformability constraints.

Table 1: Radius R, compactness C, Love number k_2, and tidal deformability Λ for $M = 1.4M_{\odot}$ NS models built with the MS1 EoS (top) and the SLy EoS (bottom), as the percentage of MDM mass varies as indicated in the table header.

M_{MDM}/M	**10%**	**20%**	**30%**	**40%**	**50%**
R [km]	13.97	13.06	12.13	11.24	10.44
C	0.148	0.158	0.170	0.184	0.198
k_2 [10^{-2}]	8.38	7.37	6.47	6.23	6.76
Λ	786	495	301	197	148
R [km]	10.90	9.98	9.06	8.22	7.57
C	0.190	0.207	0.228	0.251	0.273
k_2 [10^{-2}]	6.00	4.85	4.04	3.52	3.33
Λ	163	85	44	23	15

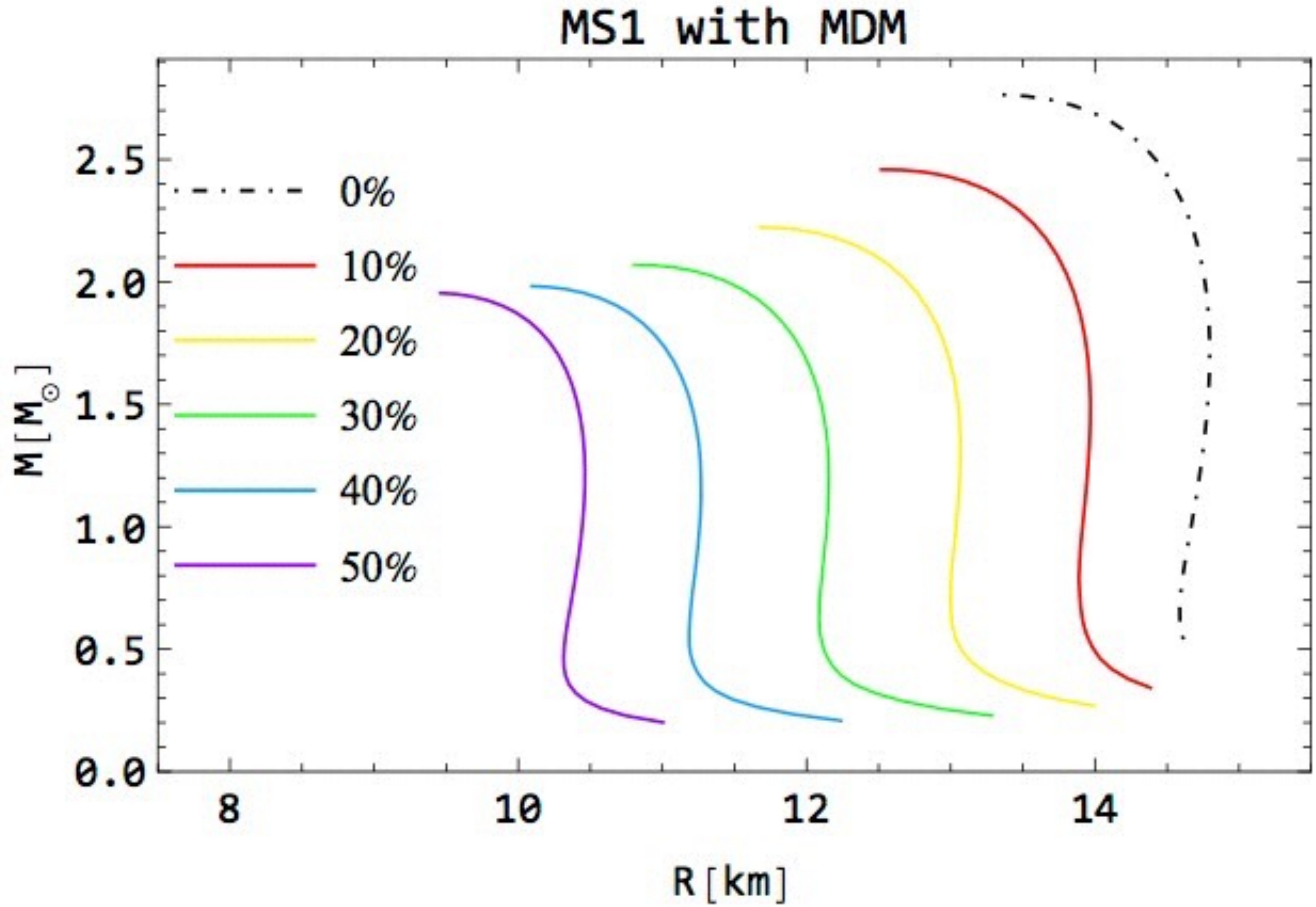
MS1 with MDM
0%
10%
20%
30%
40%
50%
M[M$_\odot$]
R[km]
0.0
0.5
1.0
1.5
2.0
2.5
8
10
12
14

Mergings of Mirror Neutron stars

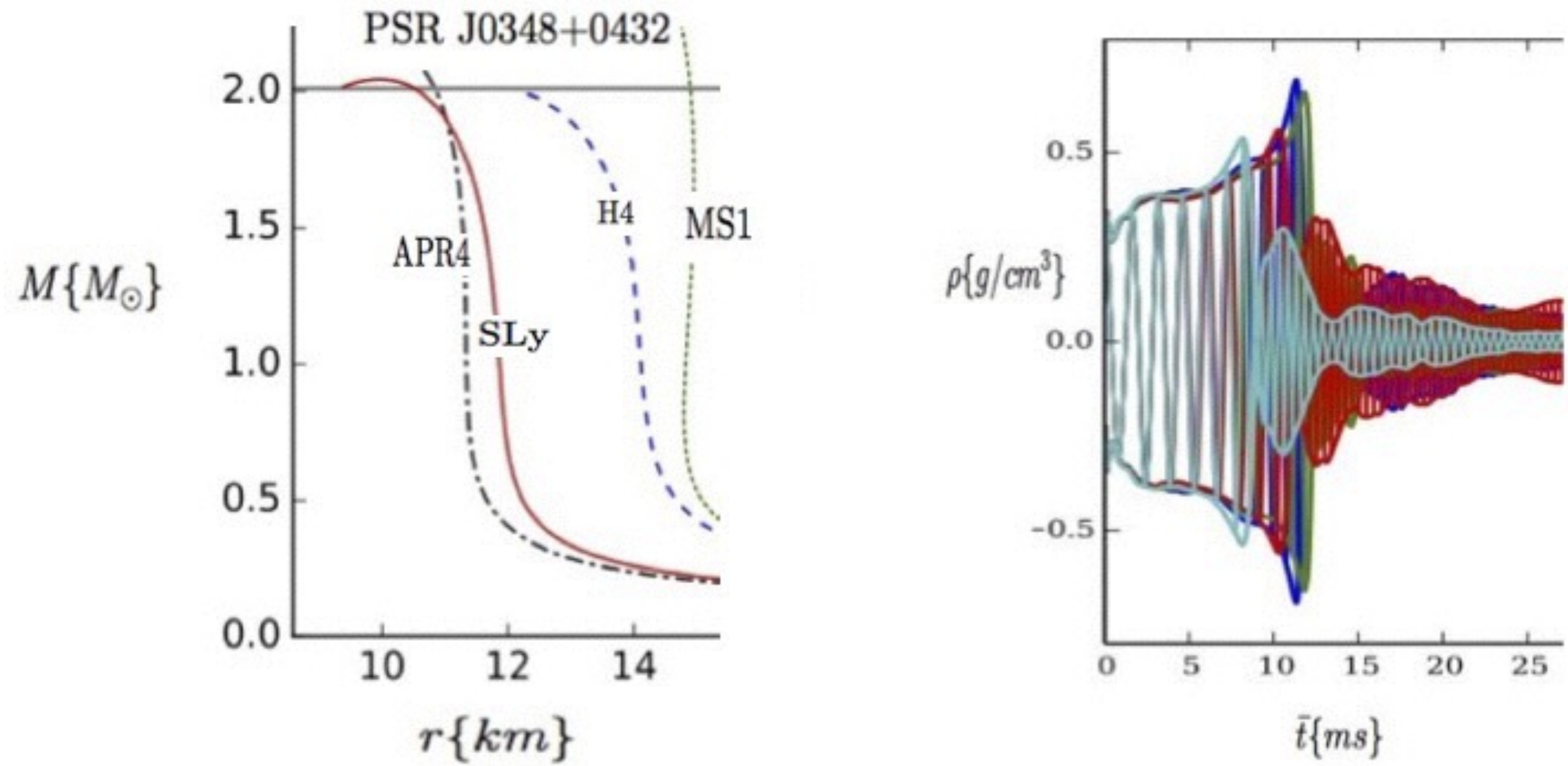

in fact, the same of Kilonovas, but not any electromagnetic counterpart (Addazi, Marciano 2017)

But not only GWs from dark objects, also possible diffuse stochastic GWs from early Universe dynamics

Mirror dark first order phase transitions and stochastic gravitational waves background

$$\frac{n_{B'}}{s'} \sim -2.4 \times 10^{-10} \kappa_s \Delta\theta'_{CP}$$

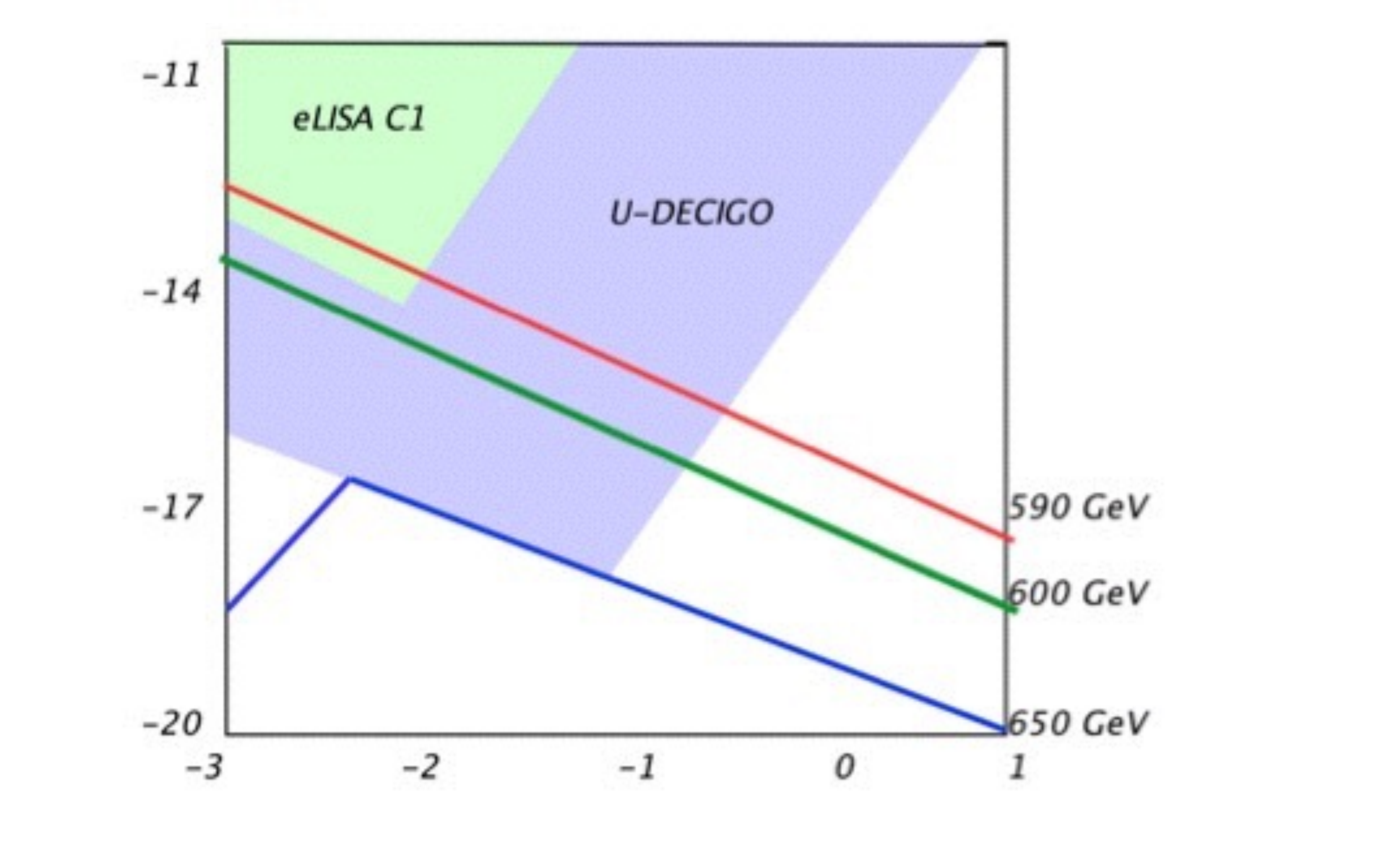

Dark Matter genesis and Gravitational waves, *Addazi (2015)*

Dark Matter direct detection. An analysis of DAMA/LIBRA signal

Asymmetric mirror DM and DAMA/LIBRA

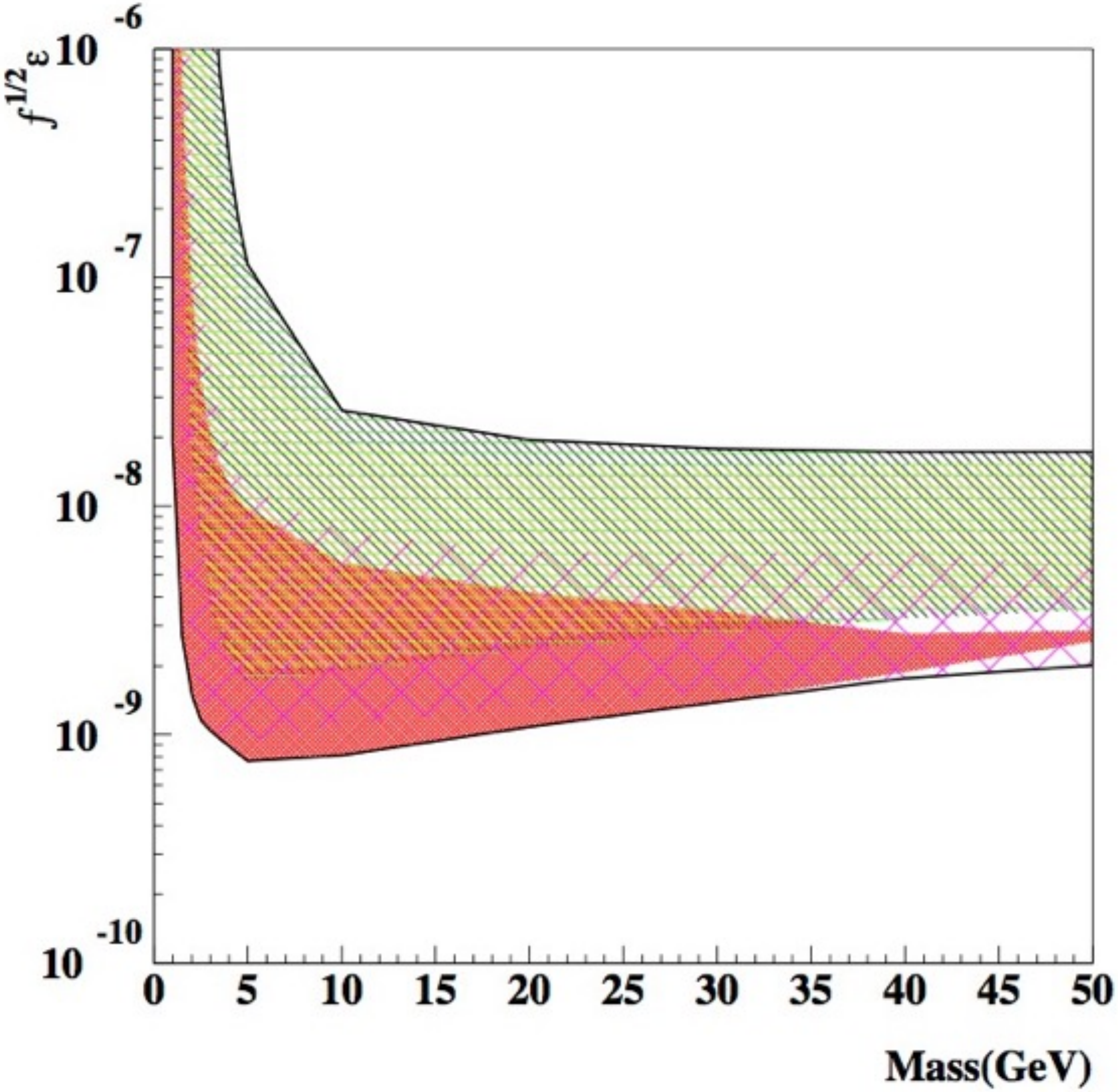

Figure 5: Allowed regions for the $\sqrt{f}\epsilon$ parameter as function of $M_{A'}$, when the assumption $M_{A'} \simeq 5m_p$ is released, obtained by marginalizing all the models for each considered scenario as given in Table 2. The $M_{A'}$ interval from few GeV up to 50 GeV is explored. These allowed intervals identify the $\sqrt{f}\epsilon$ values corresponding to C.L. larger than 5σ from the *null hypothesis*, that is $\sqrt{f}\epsilon = 0$. The five scenarios defined in Table 2 can be recognized on the basis of different hatching of the allowed regions; the black line is the overall boundary.

Range of mass and self-collisionality
compatible with Mirror Delta++
(see Addazi, Berezhiani,
Bernabei, Belli et al 2015).
Only one proton composite states stable
with v’/v high hierarchy

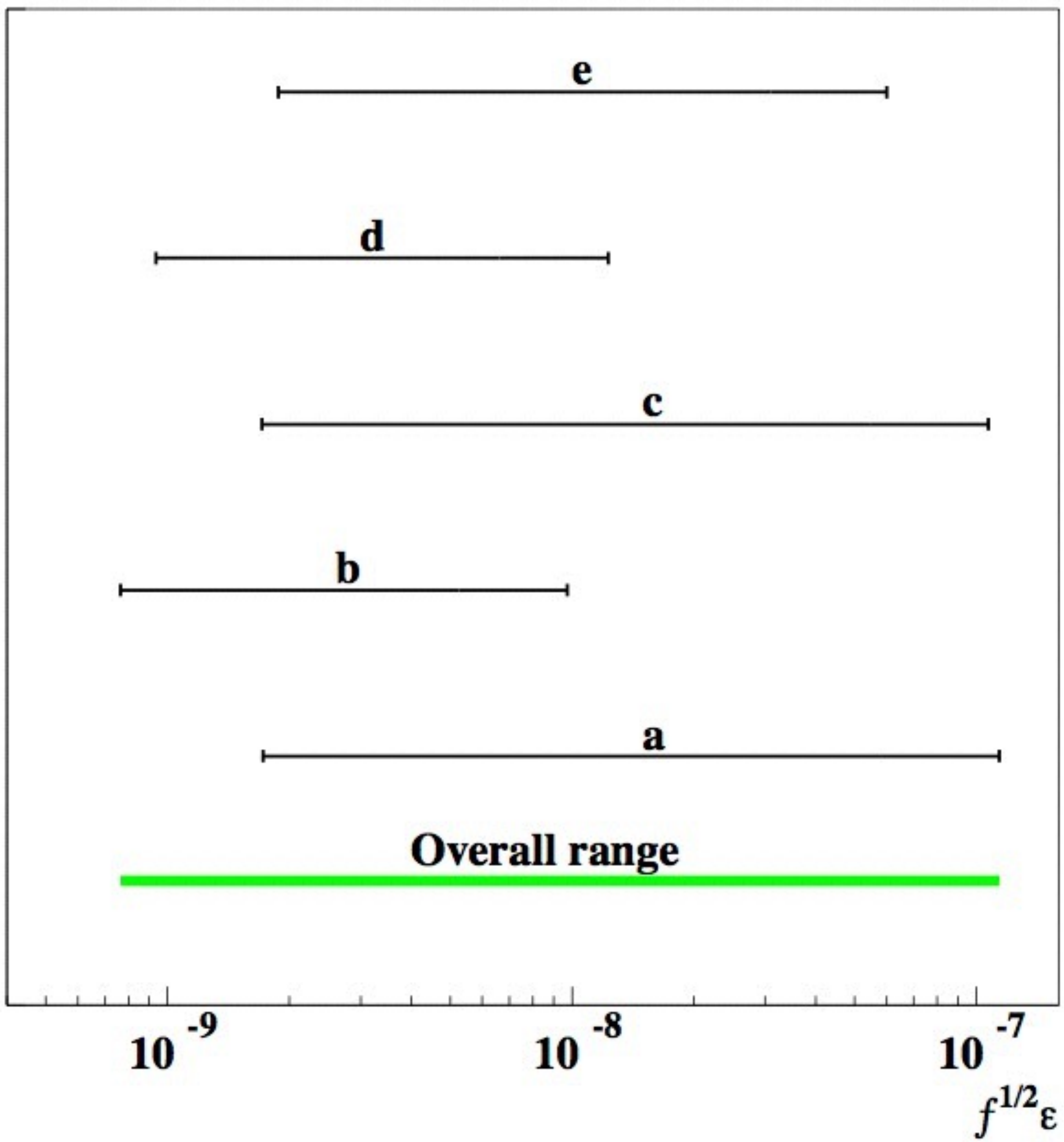

e
d
c
b
a
Overall range
10 -9
10 -8
10 -7
$f^{1/2}\varepsilon$

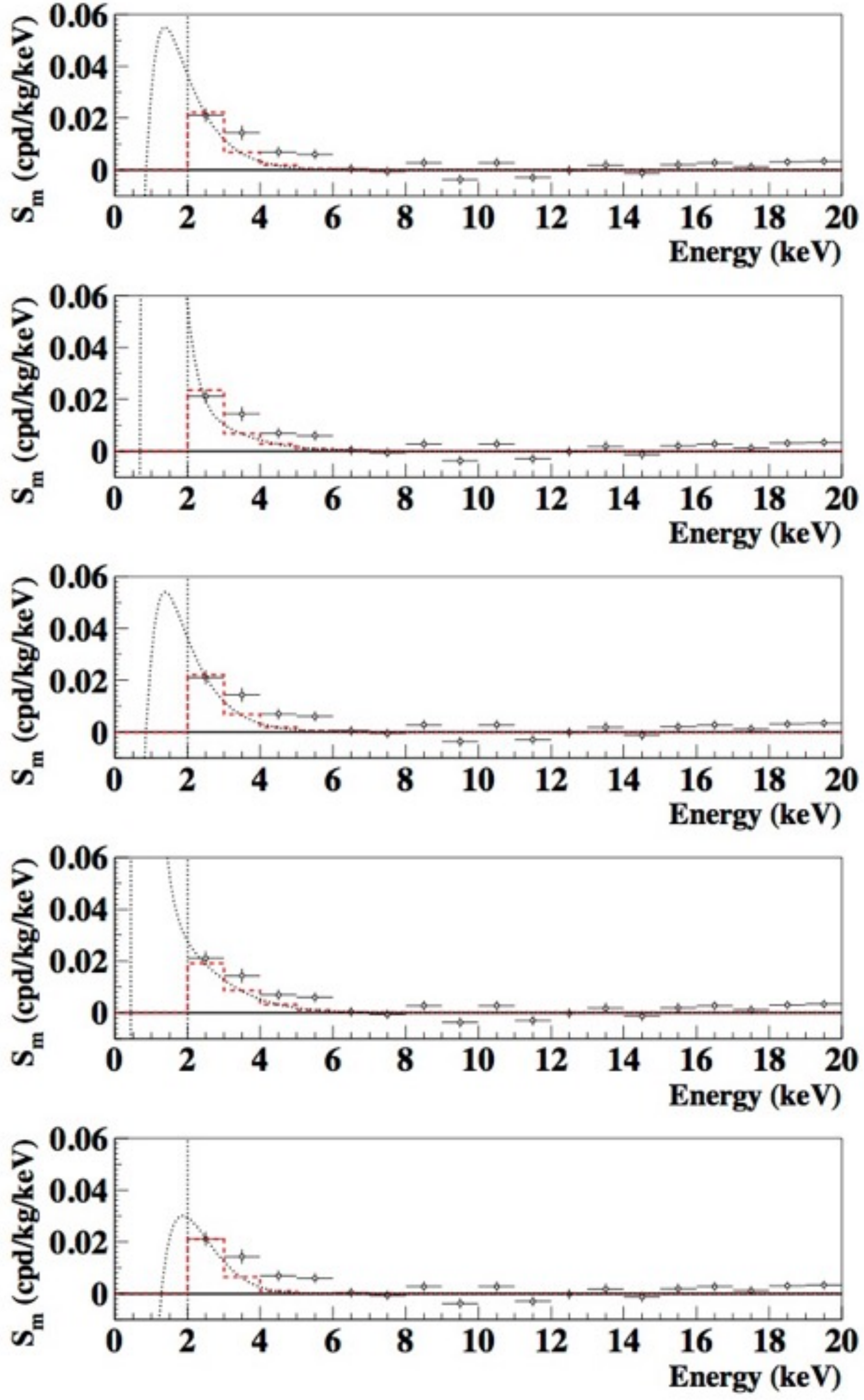

0.06
0.04
0.02
0
S_m (cpd/kg/keV)
0 2 4 6 8 10 12 14 16 18 20
Energy (keV)
0.06
0.04
0.02
0
S_m (cpd/kg/keV)
0 2 4 6 8 10 12 14 16 18 20
Energy (keV)
0.06
0.04
0.02
0
S_m (cpd/kg/keV)
0 2 4 6 8 10 12 14 16 18 20
Energy (keV)
0.06
0.04
0.02
0
S_m (cpd/kg/keV)
0 2 4 6 8 10 12 14 16 18 20
Energy (keV)
0.06
0.04
0.02
0
S_m (cpd/kg/keV)
0 2 4 6 8 10 12 14 16 18 20
Energy (keV)

Scenario	Quenching Factor	Channeling	Migdal	$\sqrt{f}\epsilon$ best	$\sqrt{f}\epsilon$ interval ($\times 10^{-9}$)
a	Q_I [4]	no	no	4.45×10^{-9} (9.2σ C.L.)	1.86–4.52 (all) 1.73–114.
b	Q_I [4]	yes	no	2.89×10^{-9} (9.3σ C.L.)	1.16–2.93 (all) 0.77–9.72
c	Q_I [4]	no	yes	4.40×10^{-9} (9.2σ C.L.)	1.85–4.47 (all) 1.72–107.
d	Q_{II} [87]	no	no	2.44×10^{-9} (9.5σ C.L.)	1.03–2.48 (all) 0.94–12.3
e	Q_{III} [87]-normalized	no	no	5.18×10^{-9} (9.0σ C.L.)	2.24–5.26 (all) 1.89–60.1

Class A: spherical $\rho_{\rm dm}$, isotropic velocity dispersion		
A0	Isothermal Sphere	
A1	Evans' logarithmic	$R_c = 5$ kpc
A2	Evans' power-law	$R_c = 16$ kpc, $\beta = 0.7$
A3	Evans' power-law	$R_c = 2$ kpc, $\beta = -0.1$
A4	Jaffe	$\alpha = 1$, $\beta = 4$, $\gamma = 2$, $a = 160$ kpc
A5	NFW	$\alpha = 1$, $\beta = 3$, $\gamma = 1$, $a = 20$ kpc
A6	Moore et al.	$\alpha = 1.5$, $\beta = 3$, $\gamma = 1.5$, $a = 28$ kpc
A7	Kravtsov et al.	$\alpha = 2$, $\beta = 3$, $\gamma = 0.4$, $a = 10$ kpc
Class B: spherical $\rho_{\rm dm}$, non–isotropic velocity dispersion (Osipkov–Merrit, $\beta_0 = 0.4$)		
B1	Evans' logarithmic	$R_c = 5$ kpc
B2	Evans' power-law	$R_c = 16$ kpc, $\beta = 0.7$
B3	Evans' power-law	$R_c = 2$ kpc, $\beta = -0.1$
B4	Jaffe	$\alpha = 1$, $\beta = 4$, $\gamma = 2$, $a = 160$ kpc
B5	NFW	$\alpha = 1$, $\beta = 3$, $\gamma = 1$, $a = 20$ kpc
B6	Moore et al.	$\alpha = 1.5$, $\beta = 3$, $\gamma = 1.5$, $a = 28$ kpc
B7	Kravtsov et al.	$\alpha = 2$, $\beta = 3$, $\gamma = 0.4$, $a = 10$ kpc
Class C: Axisymmetric $\rho_{\rm dm}$		
C1	Evans' logarithmic	$R_c = 0$, $q = 1/\sqrt{2}$
C2	Evans' logarithmic	$R_c = 5$ kpc, $q = 1/\sqrt{2}$
C3	Evans' power-law	$R_c = 16$ kpc, $q = 0.95$, $\beta = 0.9$
C4	Evans' power-law	$R_c = 2$ kpc, $q = 1/\sqrt{2}$, $\beta = -0.1$
Class D: Triaxial $\rho_{\rm dm}$ (q = 0.8, p = 0.9)		
D1	Earth on maj. axis, rad. anis.	$\delta = -1.78$
D2	Earth on maj. axis, tang. anis.	$\delta = 16$
D3	Earth on interm. axis, rad. anis.	$\delta = -1.78$
D4	Earth on interm. axis, tang. anis.	$\delta = 16$

$$\frac{d\sigma_{A,A'}}{dE_R} = \frac{\mathcal{C}_{A,A'}}{E_R^2 v^2}$$

$$\mathcal{C}_{A,A'} = \frac{2\pi\epsilon^2\alpha^2 Z^2 Z'^2}{M_A}\mathcal{F}_A^2\mathcal{F}_{A'}^2$$

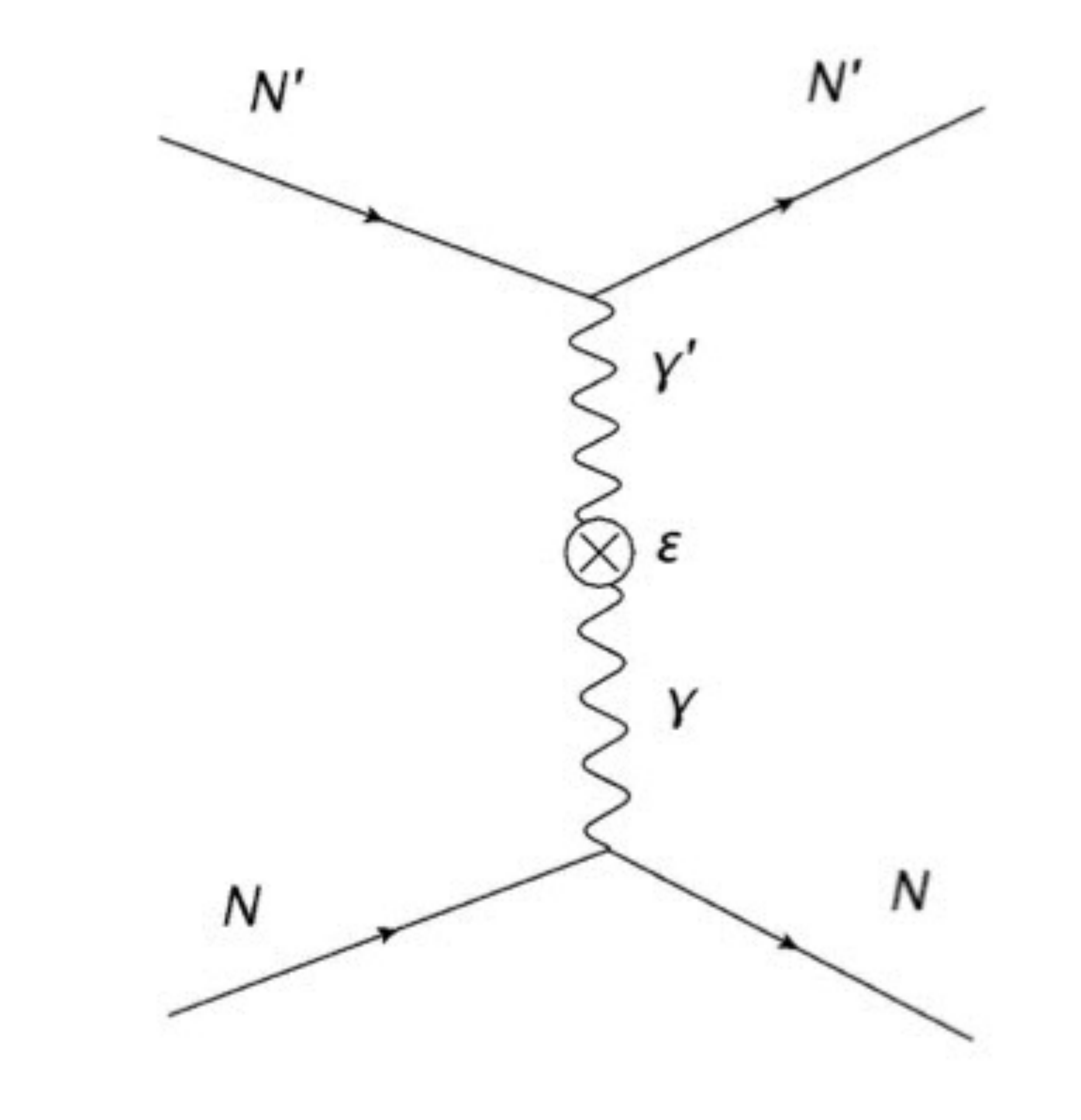

Symmetric Mirror and DAMA/LIBRA

Multi-mirror-nuclei can scatter on DAMA/LIBRA detector

Astrophysical complexity
local interstellar gas balls
with different temperatures

possible dark matter streams

Mirror matter composition	H (%)	He (%)	C (%)	O (%)	Fe (%)
H′, He′	25	75	-	-	-
H′, He′, C′, O′	12.5	75.	7.	5.5	-
H′, He′, C′, O′, Fe′	20	74	0.9	5.	0.1

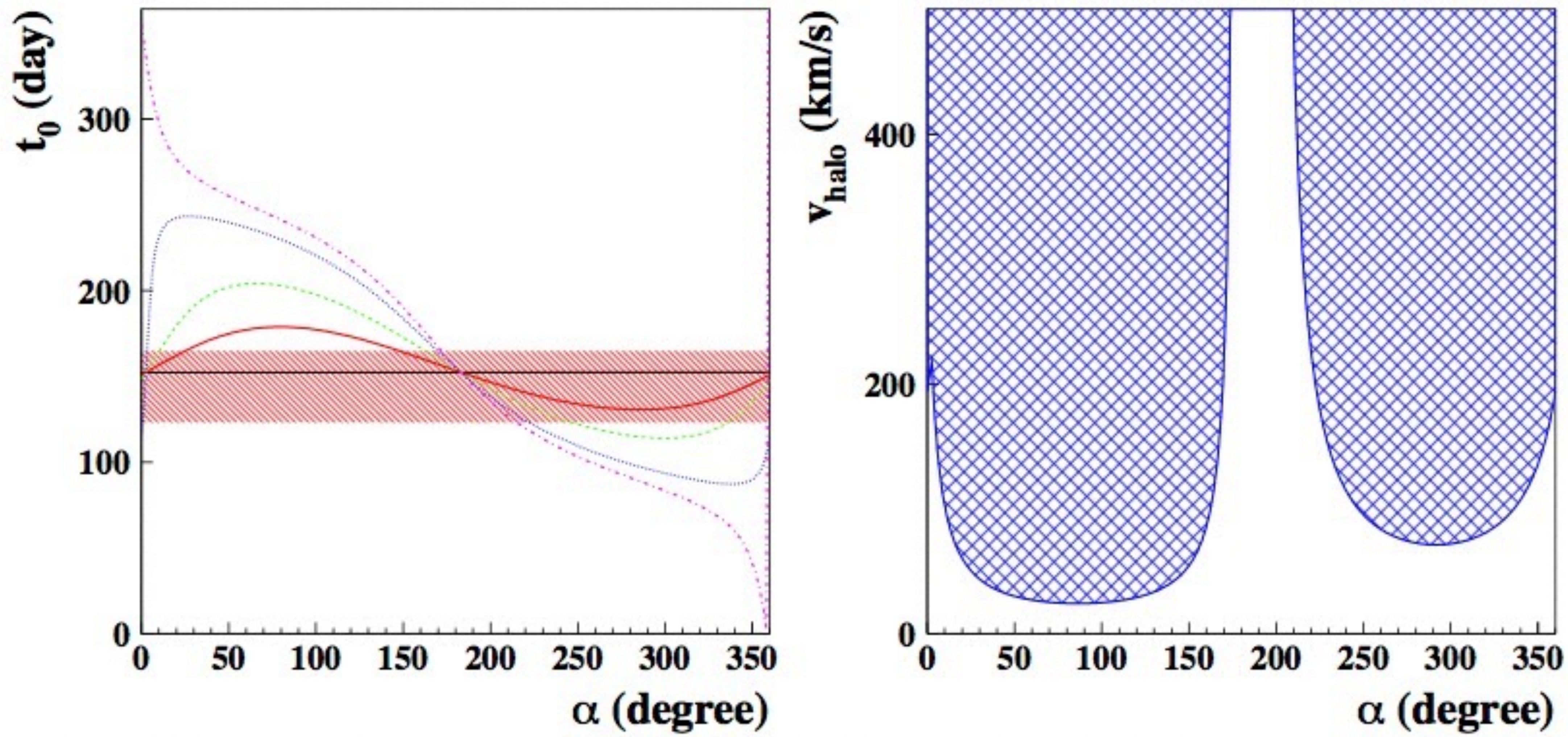

Figure 1: *Left:* examples of expected phase of the annual modulation signal as a function of the angle, α, between the Sun velocity and the velocity of the DM mirror halo moving in the Galactic plane. The different curves refer to different values of the module of the halo velocity: 300 km/s (dashed-dotted), 200 km/s (dotted), 100 km/s (dashed), 50 km/s (solid). The shaded area (red on-line) is defined by the values of the phase of the annual modulation signal allowed at 3σ by DAMA. For each halo velocity, only the values of α included inside the shaded area are allowed. The solid horizontal black line corresponds to a halo at rest in the Galactic frame ($\boldsymbol{v}_{halo} = 0$) giving a phase equal to 152.5 day (June 2^{nd}). *Right:* the shaded regions in the plane v_{halo} *vs* α correspond to halo velocities (module and direction) giving a phase that differs more than 3σ from the phase of the annual modulation effect measured by DAMA. These velocities in the shaded regions are thus excluded by the DAMA results at 3σ C.L..

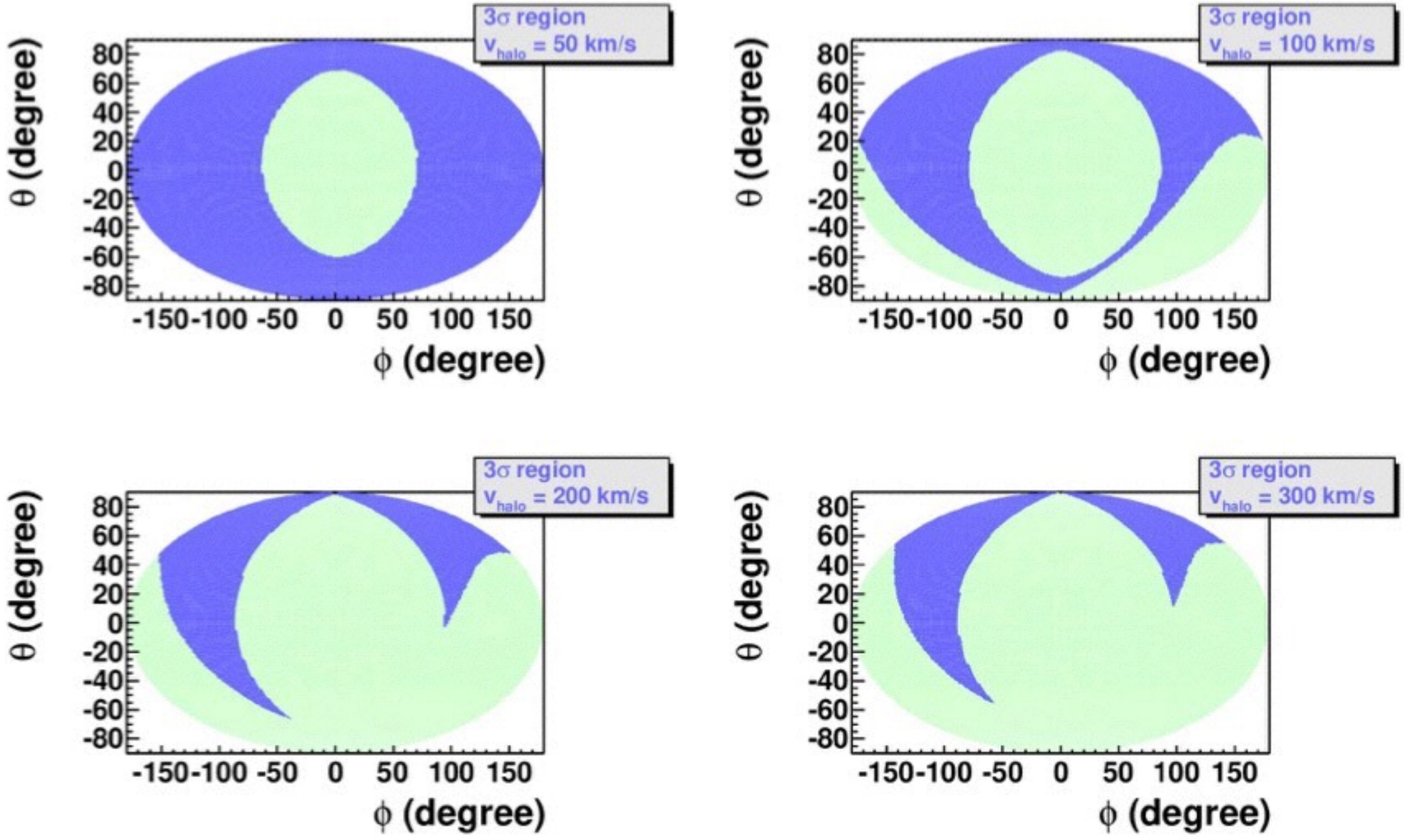

Figure 2: The dark (blue on-line) regions correspond to directions of the halo velocities in Galactic Coordinate (θ,ϕ) giving a phase compatible at 3σ C.L. with the annual modulation phase measured by DAMA. The four panels refer to different values of the velocity module: 50 km/s, 100 km/s, 200 km/s, 300 km/s.

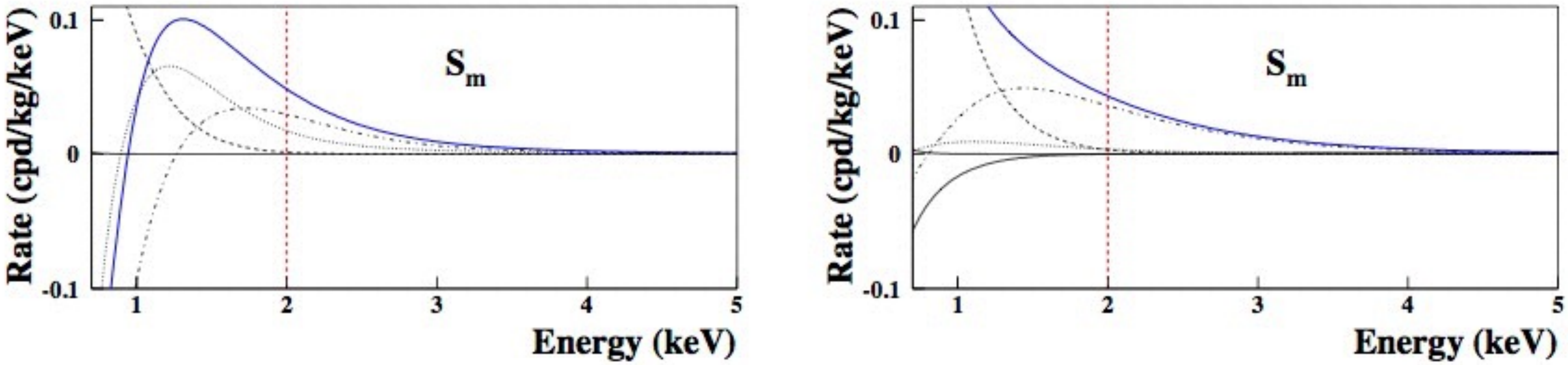

Figure 4: Examples of expected modulation amplitude, S_m, of the DM signal for the mirror DM candidates in the scenario (b) (left) and (a) (right) of Table 3, for two different halo compositions. *Left*: composite dark halo: H′(12.5%), He′(75%), C′(7%), O′(5.5%), with halo velocity $v_{halo} = 30$ km/s, temperature $T = 10^6$K, $v_0 = 220$ km/s and parameters in the set A. The contributions to the signal (solid line, blue on-line) of the different dark atoms are depicted: H′ (not visible), He′ (dashed), C′ (dotted), O' (dashed-dotted). *Right*: composite dark halo: H′(20%), He′(74%), C′(0.9%), O′(5%), Fe′(0.1%), with halo velocity $v_{halo} = 0$ km/s, temperature $T = 10^7$K, $v_0 = 220$ km/s and parameters in the set A. The contributions to the signal (solid line, blue on-line) due to the different dark atoms are depicted: H′ (solid line, visible well below 1 keV), He′ (dashed), C′ (dotted), O′ (dashed-dotted), Fe′ (solid and negative below 2 keV).

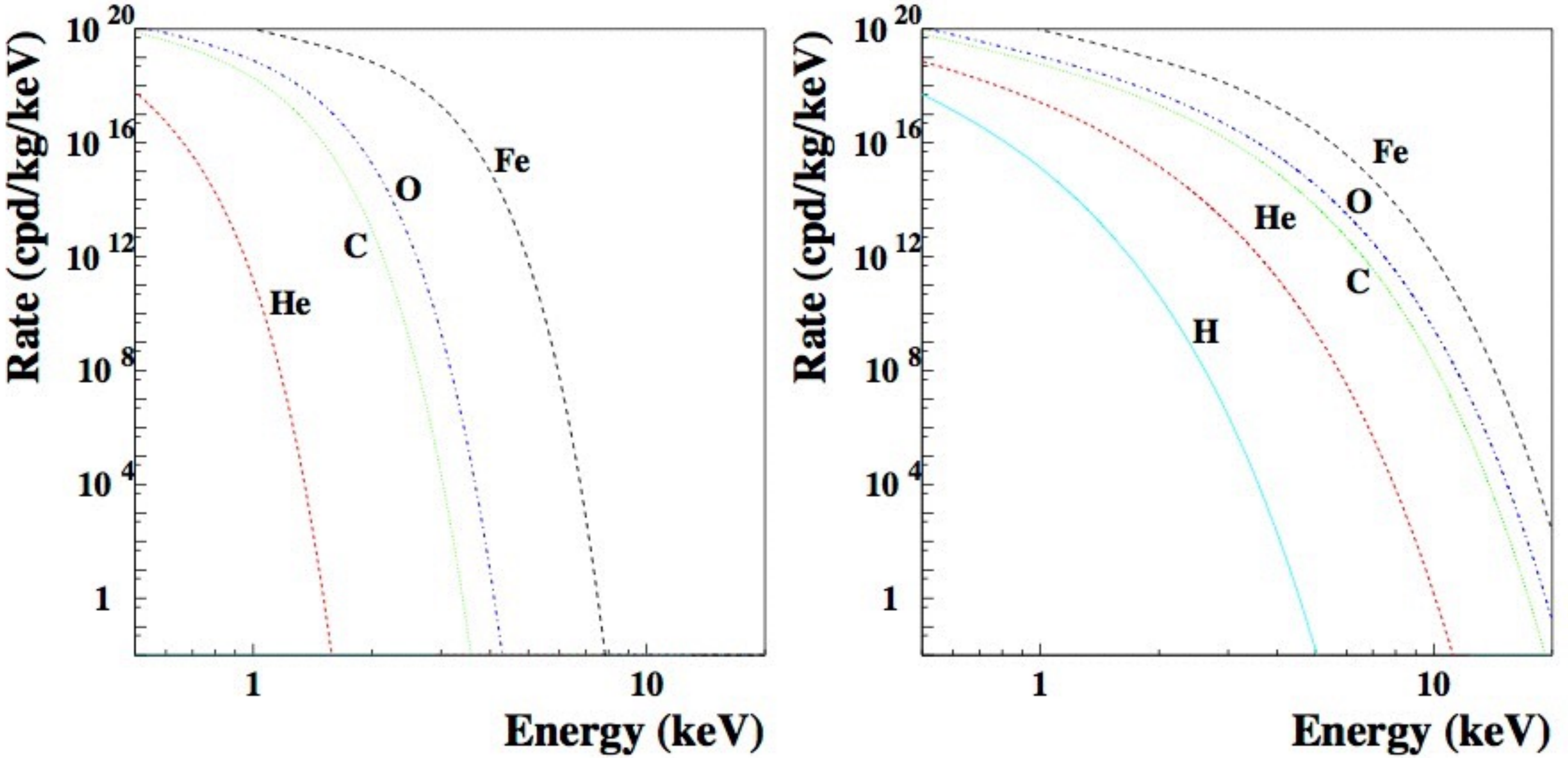

Figure 3: Constant part of the annual modulation signal expected for only one mirror atom specie in a NaI(Tl) detector, by considering $\sqrt{f}\epsilon = 1$. Few different mirror atoms are reported. The two panels refer to the case of cold ($T = 10^4$ K) (left panel) and hot ($T = 10^7$ K) (right panel) halo with $v_{halo} = 100$ km/s. The considered scenario is the case a of Table 3 in set A (see Sect. 4.4).

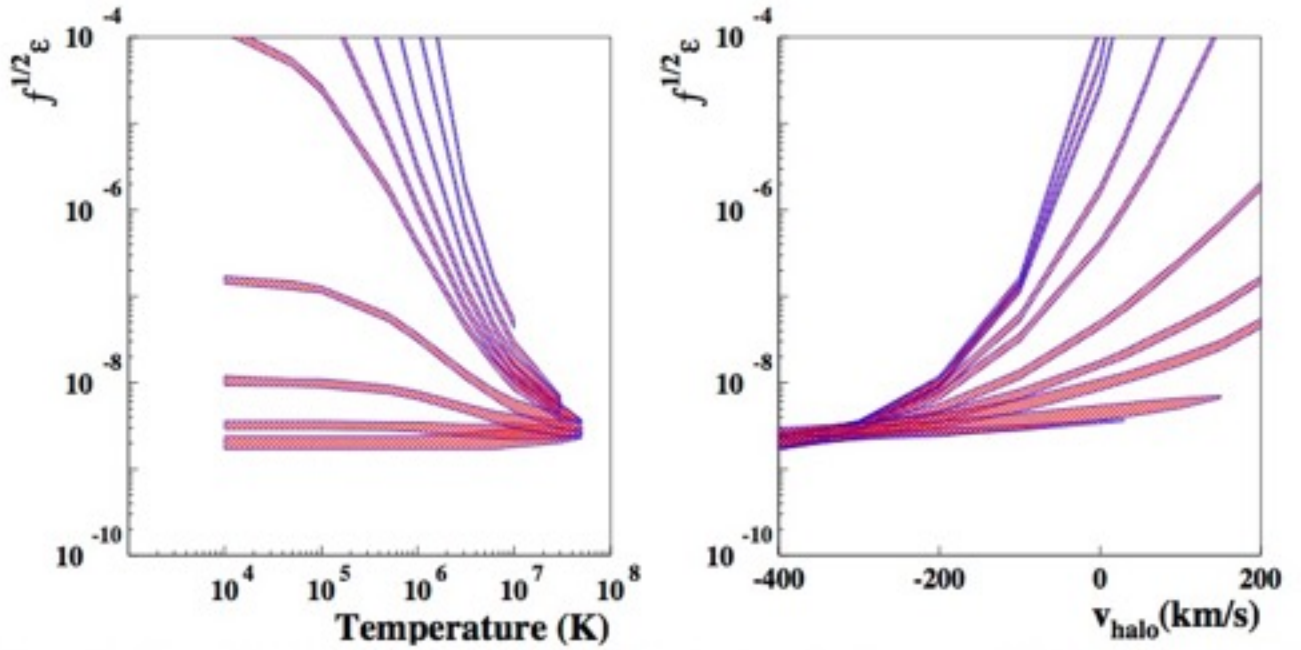

Figure 5: Case of halo composed by pure He' dark atoms in the scenario (a) of Table 3 with $v_0 = 220$ km/s and parameters in the set A (see text). *Left*: allowed regions for the $\sqrt{f}\epsilon$ parameter as a function of the halo temperature for different values of the halo velocity in the Galactic frame: -400, -300, -200, -100, 0, 30, 60, 100, 150, 200 km/s. Increasing the halo velocity the allowed regions e.g. at temperature of 10^4 K move to higher values of $\sqrt{f}\epsilon$ parameter. *Right*: allowed regions for the $\sqrt{f}\epsilon$ parameter as function of the halo velocity in the Galactic frame for different halo temperature: $10^4, 5\times10^4, 10^5, 5\times10^5, 10^6, 3.1\times10^6, 6.2\times10^6, 10^7, 3\times10^7, 5\times10^7$ K Increasing the temperature the allowed region at large positive v_{halo} move to small values of $\sqrt{f}\epsilon$ parameter. These allowed intervals identify the $\sqrt{f}\epsilon$ values corresponding to C.L. larger than 5σ from the null annual modulation hypothesis, that is $\sqrt{f}\epsilon = 0$.

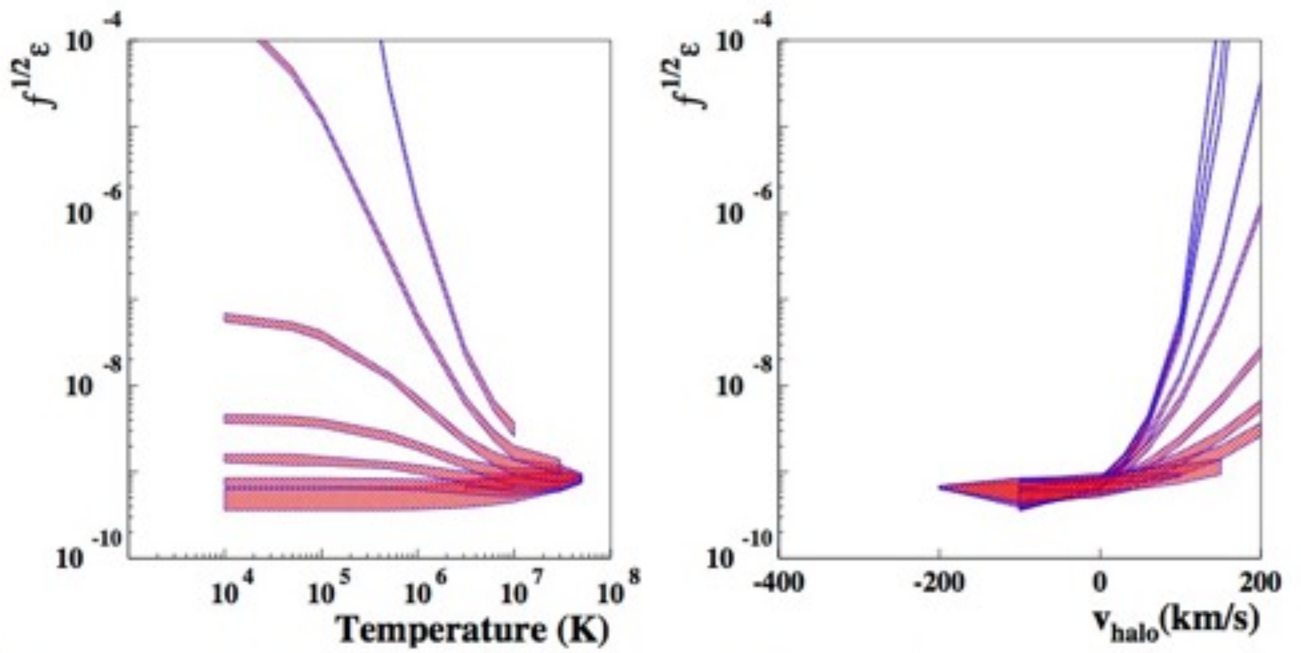

Figure 6: Case of halo composed just by pure C' dark atoms in the scenario (a) of Table 3 with $v_0 = 220$ km/s and parameters in the set A (see text and Fig. 5). The different values of the halo velocity in the left plot are: -200, -100, 0, 30, 60, 100, 150, 200 km/s. The different values of the halo temperature in the right plot are as those of Fig. 5.

Conclusions and remarks

Mirror Dark Matter has a unique phenomenology completely different from WIMPs

If Mirror matter existed, Neutron physics would be the key to unveil the dark sector

Direct detection: no in colliders but possible in underground experiments

Gravitational waves:
mergings of Mirror matter, Mirror matter trapped in ordinary stars and dark first order phase transitions

Grazie dell’attenzione!